Comprehensive assessment of real-time precise products from IGS analysis centers

Bofeng Li[*], Haibo Ge, Yuhang Bu, Yanning Zheng and Leitong Yuan

Abstract

Real-Time Precise Point Positioning (RT-PPP) has been one of the research hotspots in GNSS (Global Navigation Satellite System) community for decades. Real-time precise products of satellite orbits and clocks are the prerequisite for RT-PPP. Thus, it is of great importance to investigate the current multi-GNSS real-time precise products in State Space Representation (SSR) from different analysis centers. In this article, SSR products from 10 analysis centers are comprehensively evaluated by comparing them with the final products and performing the kinematic PPP. The results show that analysis centers CNES (Centre National D'Etudes Spatiales) and WHU (GNSS Research Center of Wuhan University) provide the most complete products with the best quality. Concerning the accuracy of real-time products for the GNSSs, the accuracies of orbit and clock products are better than 5 cm and 0.15 ns, respectively, for Global Positioning System (GPS), followed by Galileo navigation satellite system (Galileo), BeiDou-3 Navigation Satellite System (BDS-3), GLObal NAvigation Satellite System (GLONASS), and BeiDou-2 Navigation Satellite System (BDS-2). Meanwhile, the results of the RT-PPP with quad-system show that the positioning accuracies are 1.76, 1.12 and 2.68 cm in east, north, and up directions, respectively, and the convergence time to 0.1, 0.1, 0.2 m for corresponding directions is 15.35 min.

Keywords: Real-time precise point positioning (RT-PPP), State space representation (SSR), Multi-GNSS, Convergence time

Introduction

Precise Point Positioning (PPP) was firstly put forward by Zumberge et al. (1997). Since then, many efforts have been made to improve PPP performance. PPP Ambiguity Resolution (PPP-AR) is proposed to shorten the convergence time and obtain centimeter-level precision of positioning right after ambiguity fixing (Laurichesse and Mercier, 2007; Collins, 2008; Ge et al., 2008; Li et al., 2010; Chen, 2020). Multi-frequency algorithms are proposed to explore the frequency resources (Geng et al., 2013; Xin et al., 2020; Li et al., 2020). With the development of Global Navigation Satellite System (GNSS), multi-GNSS PPP are proposed for joint processing in order to improve the precision and shorten the convergence time (Cai and Gao, 2007; Li et al., 2015). The

uncombined model is proposed as an alternative to ionospheric-free model since it retains ionospheric parameters in the equations and is more rigorous (Boisits et al., 2020; Keshin et al., 2006; Liu et al., 2017). Moreover, PPP-RTK (Real-Time Kinematic) is proposed in order to overcome the bottleneck of PPP, like long convergence time (Odijk et al., 2016; Teunissen et al., 2010; Zhang et al., 2022).

For a long time, PPP was generally performed in post-processing mode because of the latency of the precise orbit and clock products. To meet the demands in high accuracy and real-time GNSS applications, the Real-Time Working Group (RTWG) was established in 2001 and the Real-Time Service (RTS) started as a Real-Time Pilot Project (RTPP) under the RTWG in 2007 (Weber et al., 2007). The RTS was operational in April 2013 with the release of a website (www.igs.org/rts) containing the links for user registration and the extensive information on the service access. RTS provides the GNSS orbit and

*Correspondence: bofeng_li@tongji.edu.cn

College of Surveying and GeoInformatics, Tongji University, Shanghai 200092, China

Li *et al. Satellite Navigation*   (2022) 3:12

Page 2 of 17

clock corrections that enable Real-Time PPP (RT-PPP) and related applications, such as time synchronization and disaster monitoring in worldwide scales (Bedford et al., 2020; Chen et al., 2020). RTS is based on the International GNSS Service (IGS) global infrastructure of network stations, data centers, and analysis centers that provide world standard high-precision GNSS data products. Currently, as shown in Table 1, there are 10 real-time Analysis Centers (AC), including Bundesamt für Kartographie und Geodäsie (BKG), the Institute of Geodesy and Geophysics (IGG) of Chinese Academy of Sciences (CAS), Centre National d'Etudes Spatiales (CNES), Deutsches Zentrum für Luft-und-Raumfahrt (DLR), European Space Agency (ESA), GeoForschungsZentrum (GFZ), GMV Aerospace and Defense (GMV), Natural Resources Canada (NRCan), Shanghai Astronomical Observatory (SHAO), and GNSS Research Center of Wuhan University (WHU). Here SHAO is not presented since its mount-point is not found from casters during the experimental period (Feb. 2021). With the development of RTS, RT-PPP has been a research hotspot due to the high demand of real-time users. The positioning accuracy of RT-PPP with RTS can be improved by 50% in comparison to that with IGS ultra-rapid products (Elsobeiey & Al-Harbi, 2016). Zhang et al. (2018) indicated that the accuracy of only Global Positioning System (GPS) RT-PPP can be better than 10 cm in each coordinate direction. With the development of other global systems, multi-GNSS RT-PPP has attracted the great interests of many researchers because of the increase in the number of satellites as well as the enhancement of satellite distribution geometry (de Bakker and Tiberius, 2017; Krzan and Przestrzelski, 2016). The multi-GNSS RT-PPP was investigated with a combination of two systems (Liu et al., 2018) to four systems (Kazmierski et al., 2018; Wang et al., 2018a, b). The convergence time can be improved by 30, 42 and 35%, respectively and positioning accuracy by 26, 30 and 22%, respectively, in three coordinate directions with GPS, GLObal NAvigation Satellite System (GLONASS), BeiDou-2 Navigation Satellite System (BDS-2) in comparison to the GPS-only RT-PPP (Abdi et al., 2017).

The multi-GNSS RT-PPP undoubtedly can greatly improve the positioning accuracy and shorten the convergence time. However, the RTS is currently offered only for GPS, while multi-GNSS products are still in the stage of developing and testing. Thus, different ACs provide different RTS products, as shown in Table 1. Most research is focused on the analysis of the RTS products from one AC but few on the performance of the RTS products from different ACs. Wang et al., (2018a, b) assessed multi-GNSS real-time products from IGS RTS, including GPS, GLONASS, Galileo navigation satellite system (Galileo), and BeiDou Navigation Satellite System (BDS). However, real-time products of BeiDou-3 Navigation Satellite System (BDS-3) was not evaluated since it is still under construction at that time (Zhang et al., 2019). Thus, it is necessary to comprehensively investigate the quality of current multi-GNSS RTS products from different ACs as well as their performances in multi-GNSS RT-PPP.

In this study, the RTS will be briefly introduced, including the format of real-time products and the transmission protocol. Then the algorithm of recovering real-time products for the PPP-users is elaborated. Next, the accuracies of real-time products from different ACs will be analyzed by comparing them with post-processed products. Currently, many ACs provide multi-GNSS post-processed products, where the precision of products from different ACs is consistent with each other, while the products of GFZ and WHU are more complete than those of other ACs, especially for BDS (Montenbruck

Table 1 Details of mount-points of each AC (detailed naming convention of the mount-points can be referred to Table 2. Supported systems: G, R, E, and C denote GPS, GLONASS, Galileo, and BDS, respectively.)

ACs	Mount-points	Supported systems	Broadcast interval for orbit and clock corrections (s)	Code bias provided	Phase bias provided
IGS	SSRA03IGS0	GREC	60, 5		
CNES	SSRC00CNE0	GREC	5, 5	Yes	Yes
WHU	SSRC00WHU0	GREC	5, 5		
DLR	SSRC00DLR1	GREC	30, 5		
BKG	SSRC00BKG0	G	60, 5		
NRCan	SSRA00NRC0	G	5, 5		
ESA	SSRC00ESA1	G	5, 5		
GFZ	SSRC00GFZ0	GREC	5, 5	Yes	
GMV	SSRC00GMV0	GRE	5, 5 (10, 10)	Yes	
CAS	SSRC00CAS0	GREC	5, 5		

et al., 2017). Though WHU has many research on orbit models of BDS (Wang et al., 2019; Zhao et al., 2017), we cannot find the orbit models applied by WHU, especially for solar radiation pressure model. Thus, precise post-processed products from GFZ are selected as the reference in order to assess the internal accuracy of real-time orbit and clock products from different ACs. Afterwards, one-week kinematic RT-PPP results are examined to evaluate the quality of real-time products with 14 Multi-GNSS Experiment (MGEX) stations. Finally, some conclusions are given.

RTS implementation

Traditional PPP is generally post-processed due to the latency of precise orbit and clock products, which is the key limitation for RT-PPP. In the RTS, ACs provide the real-time orbit and clock corrections with respect to the navigation messages according to the Radio Technical Commission for Maritime Services (RTCM) 10,403.x protocols. These corrections are broadcasted to global users via internet based on Networked Transport of RTCM via Internet Protocol (NTRIP) with very low latency. Thus, the format of real-time products and the usage of NTRIP are of great importance for real-time users. In this section, the format of RTCM and NTRIP will be briefly introduced.

In order to establish and maintain the standards and protocols of real-time products, IGS joined the RTCM Special Committee (RTCM-SC) 104 in 2008 and released "RTCM STANDARD 10,403.1" for real-time products. However, only GPS and GLONASS are supported with the real-time products at that time. For further standardization and unification of the products of different GNSSs, IGS released the "IGS State Space Representation (SSR) Format V1.0" in Oct. 2020 (https://www.igs.org/formats-and-standards). This standard supports not only the four global GNSS systems, but also the regional systems of Quasi-Zenith Satellite System (QZSS) and Satellite Based Augmentation Systems (SBAS).

NTRIP, consisting of server, caster and client, is recommended as the standard transmission protocol of RTCM. As a kernel component, the caster is responsible for not only receiving real-time products from the servers of ACs, but also responding the users' requests of real-time products from the client (Standard, 2011). Thus, the real-time users need to know the instructions about the caster and the client. Currently, there are 10 casters providing RTCM-SSR products. For each caster, users can choose different mount-points for real-time products from different ACs. In 2019, RTWG announced a new naming convention of "TTTTXXAAAF" in Table 2 (https://igs.bkg.bund.de/ntrip/).

Algorithm of recovering real-time products

IGS ACs broadcast real-time products in the format of RTCM-SSR. Compared to Observation State Representation (OSR), SSR consists of more correction details and can be globally applied thanks to its location-independence. The orbit and clock products provided by IGS ACs are essentially the corrections with respect to the broadcast counterparts. Therefore, this section will mainly introduce how to use SSR products to recover high-precise orbit and clock products.

Recovery of precise orbit products

The IGS real-time orbit corrections in SSR include the satellite position correction $d\boldsymbol{O} = \begin{bmatrix} \delta O_r & \delta O_a & \delta O_c \end{bmatrix}^T$ in the spacecraft body fixed system at reference time t_0 and the satellite velocity correction $d\dot{\boldsymbol{O}} = \begin{bmatrix} \delta \dot{O}_r & \delta \dot{O}_a & \delta \dot{O}_c \end{bmatrix}^T$. Then the orbit corrections at epoch t is calculated as

$$\delta \boldsymbol{O} = d\boldsymbol{O} + d\dot{\boldsymbol{O}}(t - t_0) \tag{1}$$

Since the positioning is usually conducted in Earth-Centered- Earth-Fixed (ECEF) system, one needs to convert the orbit corrections from the spacecraft body fixed system to ECEF system using a coordinate transformation:

$$\delta \boldsymbol{X} = \begin{bmatrix} \frac{\dot{r}}{|\dot{r}|} \times \frac{r \times \dot{r}}{|r \times \dot{r}|} & \frac{\dot{r}}{|\dot{r}|} & \frac{r \times \dot{r}}{|r \times \dot{r}|} \end{bmatrix} \delta \boldsymbol{O} \tag{2}$$

where $r = X_{brdc}$ and $\dot{r} = \dot{X}_{brdc}$ are the satellite position and velocity calculated by using broadcast ephemeris. The precise satellite position X_{pre} is obtained by

Table 2 Latest naming convention of the mount-points of NTRIP RTCM-SSR product

Components	Details
TTTT	Product type (SSRA: Antenna phase center SSR product; SSRC: Center-of-mass SSR product; IONO: Real-time ionosphere product)
XX	Different schemes of SSR service of a same AC
AAA	AC name
F	Format (0: RTCM 10,403.x; 1: IGS SSR Format V1.0)

$$X_{\text{pre}} = X_{\text{brdc}} - \delta X \tag{3}$$

For Geostationary Earth Orbit (GEO) satellites, the velocity $\dot{r}_{\text{GEO}}$ is computed as

$$\dot{r}_{\text{GEO}} = \dot{X}_{\text{brdc}} + \left[-\dot{\Omega}_e Y_{\text{brdc}} \ \ \Omega_e X_{\text{brdc}} \ \ 0 \right]^{\text{T}} \tag{4}$$

where $\dot{\Omega}_e = 7.2921151467 \times 10^{-5} \text{rad/s}$ is the angular velocity of earth around the Z axis.

Recovery of precise clock products
Similar to the orbit corrections in SSR, the real-time corrections of clock error are the differences between the precise clock error δt_{pre} and the clock error δt_{brdc} computed with broadcast ephemeris. However, different from orbit corrections, the correction of clock error in SSR is represented by three second-order polynomial coefficients, c_0, c_1, c_2 at reference time t_0. Then the correction of clock error δc at the epoch time t is

$$\delta c = c_0 + c_1(t - t_0) + c_2(t - t_0)^2 \tag{5}$$

Finally, the precise clock error δt_{pre} is

$$\delta t_{\text{pre}} = \delta t_{\text{brdc}} - \delta c/C_{\text{light}} \tag{6}$$

where δt_{brdc} is the clock error calculated by broadcast ephemeris. C_{light} represents the speed of light.

Currently, two types of broadcast ephemerides are available for BDS and Galileo for different frequencies, which are D1/D2 for B1I and B2I, CNAV1/CNAV2 for B1c and B2a for BDS and I/NAV for E1/E5b and F/NAV for E1/E5a for Galileo (CSNO, 2016; European Union, 2010). Users should select the broadcast ephemeris in terms of its data source IDentity (ID.)At present, the broadcast ephemeris used for BDS and Galileo SSR are mostly D1/D2 and I/NAV, respectively. In addition, the Issue of Data Ephemeris (IODE) for GPS and Galileo can be directly obtained by decoding broadcast ephemeris while for GLONASS and BDS, it is calculated as (IGS RTWG, 2020)

$$T_{\text{IODE}}^R = \text{INT}\left(\frac{1}{900} \times \text{FMOD}((T_{\text{TOC}} + 10800), 86400) \right.$$
$$\left. + 0.5 \right) \tag{7}$$

$$T_{\text{IODE}}^C = \text{FMOD}\left(\frac{T_{\text{TOES}}}{720}, 240 \right) \tag{8}$$

where T_{IODE}^R and T_{IODE}^C are the IODE for GLONASS and BDS, respectively. T_{TOC} is the reference time of GLONASS clock error. T_{TOES} is the second of week converted from the reference time of BDS clock, INT is the integer operator, and FMOD represents mod function. The

detailed information can be referred to BKG Ntrip Client (https://igs.bkg.bund.de/ntrip/download) and the RTCM 10,403 standard (RTCM Special Committee, 2016).
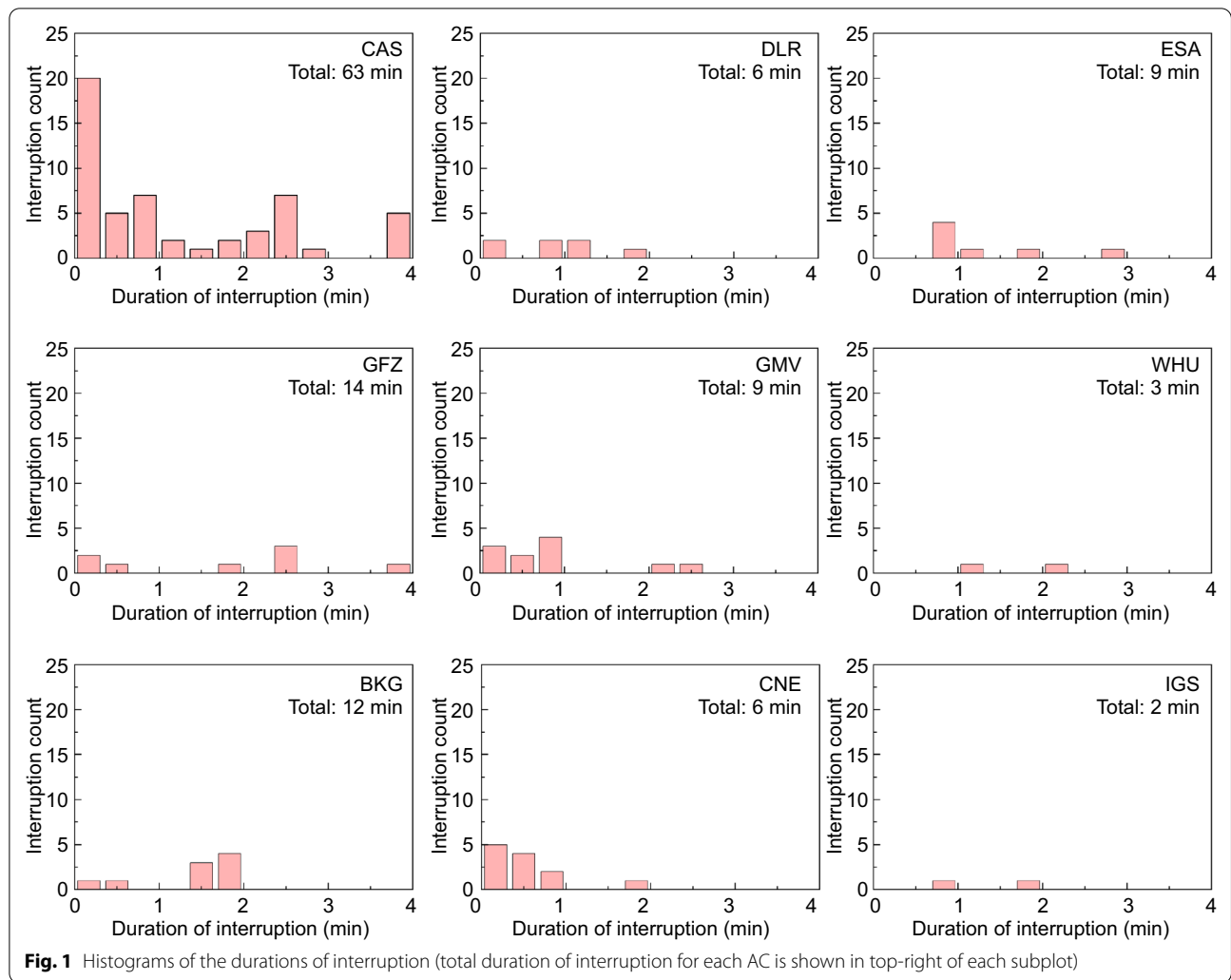
Accuracy evaluation of real-time products
The performance of RT-PPP is highly dependent on the quality of real-time SSR products. Thus, it is of great importance to systematically evaluate the quality of real-time products from different ACs. The mount-points of each AC shown in Table 1 are setup to receive one-week real-time products, from Day of Year (DOY) 31 to 37 in 2021. The interruptions during the reception of corrections are plotted in Fig. 1. Note that frequent interruptions during the test period have occurred for the products from CAS. Therefore, the products from CAS are not included for the following experiments. The GBM post-processed orbit and clock products from GFZ are taken as references (Deng et al., 2017). The following details are considered in the comparisons.

1. The sampling interval are set to 5 min and 30 s for orbit and clock corrections, respectively.
2. For some ACs, the precise satellite positions recovered with their SSR corrections are referred to the antenna reference points. However, the post-processed orbits from GFZ are all referred to the mass centers of satellites. In such a case, the satellite antenna file (igs14.atx) is applied to correct the satellite positions from ACs.
3. The clock products provided by different ACs contain corresponding singularity-basis, which could be different with different ACs. In order to eliminate this inconsistency among the time references of different clock products, the between-satellite-differenced clock errors are evaluated (Lou, 2008).
4. To eliminate the influence of gross errors on the statistical results, the results with three-dimensional orbit errors larger than 10 m for GEO satellites and 2 m for other satellites are excluded in the following analysis.

GPS real-time products
Figure 2 shows the Root Mean Square (RMS) values for each GPS satellite in along-track, cross-track, and radial directions from all ACs. Except that the orbit products of G04, G14 and G18 satellites are not provided from IGS03, all ACs provide the orbit corrections for all GPS satellites. Overall, the accuracy of real-time GPS orbits reaches a centimeter level for all ACs. The RMSs in radial direction are smaller than those in the cross-track, while those in the along-track are the largest. This is the common phenomenon in GNSS orbit since the observation

Li *et al. Satellite Navigation*   (2022) 3:12

Page 5 of 17

Fig. 1 Histograms of the durations of interruption (total duration of interruption for each AC is shown in top-right of each subplot)

directions are mostly around the radial direction rather than for the cross-track and along-track directions. The RMSs in the radial from most ACs are around 0.02 m except GFZ and GMV where it is at the level of 0.04 m. Note that the RMS of G20 is significantly larger than that of other satellites for all ACs, which may be due to the maneuvering characteristics of G20 satellite.

For the evaluation of clock products, we selected the satellite G01 as the reference satellite, where the reference satellite can be selected randomly since the choice of the reference satellite has nearly no effect on the result. Figure 3 shows the Standard Deviations (STD) of GPS satellite clock errors for different ACs. The clock products from CNES are the best with mean STD of about 0.1 ns for all GPS satellites, while they are the worst from IGS03 and DLR with the mean STD of 0.214 ns and 0.284 ns, respectively. Zero-difference integer ambiguity fixing is adopted for real-time products from CNES (Laurichesse et al., 2009), while for other ACs generally use

float solution. This is the main reason that CNES clock products are more precise.

Galileo real-time products

Six ACs, i.e., IGS, CNES, DLR, GFZ, GMV, and WHU provide Galileo real-time products (see Table 1). However, the systematic biases are found for IGS03, i.e., 1.1 m for GLONASS, 0.7 m for Galileo, and 1.4 m for BDS, which may be caused by the anomalies when synthesizing real-time clock products from each AC. Hence, the mountpoint IGS03 will not be taken into account in the following comparison of GLONASS, Galileo, and BDS.

Figure 4 shows the RMSs of Galileo orbit products in along-track, cross-track, and radial directions, respectively. The ACs CNES and DLR provided the real-time orbit products for 24 satellites, while GFZ and GMW did not for the satellites of E14 and E18 and WHU also not for the satellites of E24, E25, E26, and E36. In theory, ACs should provide precise products for all satellites in

Li *et al. Satellite Navigation*   (2022) 3:12

Page 6 of 17

Fig. 2 The RMS values in the radial (*R*), along-track (*A*), and cross-tracks (*C*) directions of GPS real-time orbit from different IGS ACs (mean RMS of orbit errors for all GPS satellites is shown in each subplot)

real time. However, many events may cause the product incomplete, such as the interruptions of correction stream as shown in Fig. 1 as well as different quality control methods adopted by different ACs. All ACs can provide real-time orbit products at centimeter level, among which CNES outperforms the others, i.e., 2.6, 4.2 and 3.2 cm for radial, along-track, and cross-track directions, respectively.

Figure 5 shows the STDs of Galileo clock errors from five ACs with E01 as the reference. The result of CNES has the best quality with the mean STD of 0.107 ns. The mean STD is 0.132, 0.148 and 0.191 ns for the products from GMV, DLR and GFZ, respectively, while the worst one is from WHU with STD of 0.238 ns.

GLONASS real-time products
Figure 6 shows the RMSs of GLONASS real-time orbits in radial, along-track, and cross-track directions, which are provided by CNES, DLR, GFZ, GMV, and WHU.

Only 18 GLONASS satellites were available, and five satellites (from R08 to R11 and R23) were invalid in the test period (https://www.glonass-iac.ru/en/cus/). Generally, the orbit RMSs of GLONASS are larger than those of GPS and Galileo in all three directions due to the difficulty in GLONASS ambiguity resolution (float ambiguities are usually adopted for GLONASS) (Li et al., 2015). The orbit accuracies from different ACs are comparable, with the RMS of about 10 cm in the along-track and 4 cm in the radial.

Figure 7 shows the STD values of GLONASS real-time clock errors provided by CNES, DLR, GFZ, GMV, and WHU with R01 as reference satellite. The mean STD is much larger than that of Galileo and GPS. The large STD is mainly due to the poor performance of GLONASS's cesium atomic clock. Comparing the results from ACs, the smallest STD of clock errors is from CNES, while the largest STD from WHU. They are 0.41 and 0.65 ns, respectively.
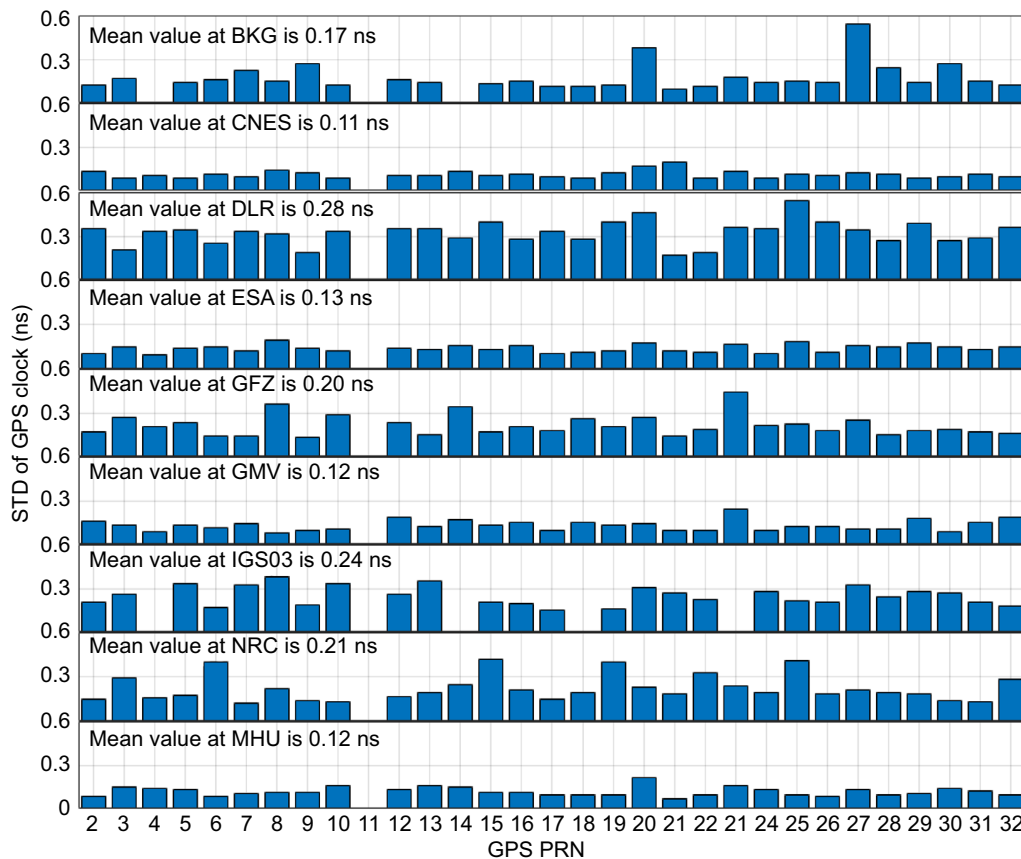
Fig. 3 The STDs of real-time GPS clock errors from different ACs with G01 as reference (mean STD of clock errors for all GPS satellites is shown in each subplot)

BDS real-time products

In the testing period, four ACs provided BDS real-time products, including CNES, DLR, GFZ, and WHU. Specifically, WHU provided the products of 41 BDS satellites and CNES 31 satellites. However, GFZ only provided the products of BDS-2 satellites (from C01 to C16), while DLR only provided products of some BDS-3 satellites (from C19 to C37). In order to comprehensively analyze the real-time SSR products, they were separately compared for GEO, Inclined Geosynchronous Orbit (IGSO), and Medium Earth Orbit (MEO) satellites of BDS-2 and BDS-3. In the evaluation of clock errors, C16 was selected as the reference for BDS-2 and C37 for BDS-3.

Figure 8 shows the RMSs of BDS-2 real-time orbits in radial, along-track, and cross-track directions provided by CNES, GFZ, and WHU. The accuracies of BDS-2 orbits are comparable among three ACs, though they had different satellite types. GEO satellites shows the largest RMS values at meter level in the along-track and the cross-track directions and decimeter level in the radial direction. For IGSO satellite, the RMS is at centimeter level in the radial direction and decimeter level in both along-track and cross-track directions. For MEO satellites, the RMS is at centimeter level for all directions.

For BDS-3, WHU provided the most complete and best real-time products, as shown in Fig. 9. The RMSs are 5.1, 9.6 and 6.0 cm for MEO satellites, and 0.17, 0.24 and 0.23 m for three IGSO satellites (from C38 to C40) in radial, along-track, and cross-track directions, respectively. Obviously, the accuracy of BDS MEO orbits is lower than that of GPS and Galileo. In past several years, many studies have carried out to refine the BDS satellites' yaw attitude and solar radiation pressure model (Dai et al., 2015; Wang et al., 2018a, 2018b; Zhao et al., 2017) that both have great impacts on the orbit quality. However, the refined models are still not as precise as those used in GPS satellites, and the specific implementation strategies of these models by different ACs are not mentioned in the file of "analysis strategy summary" (https://files.igs.org/pub/center/analysis/). It implies that the different ACs may apply the different dynamic models. This inconsistence could cause the lower accuracy of BDS MEO orbits.
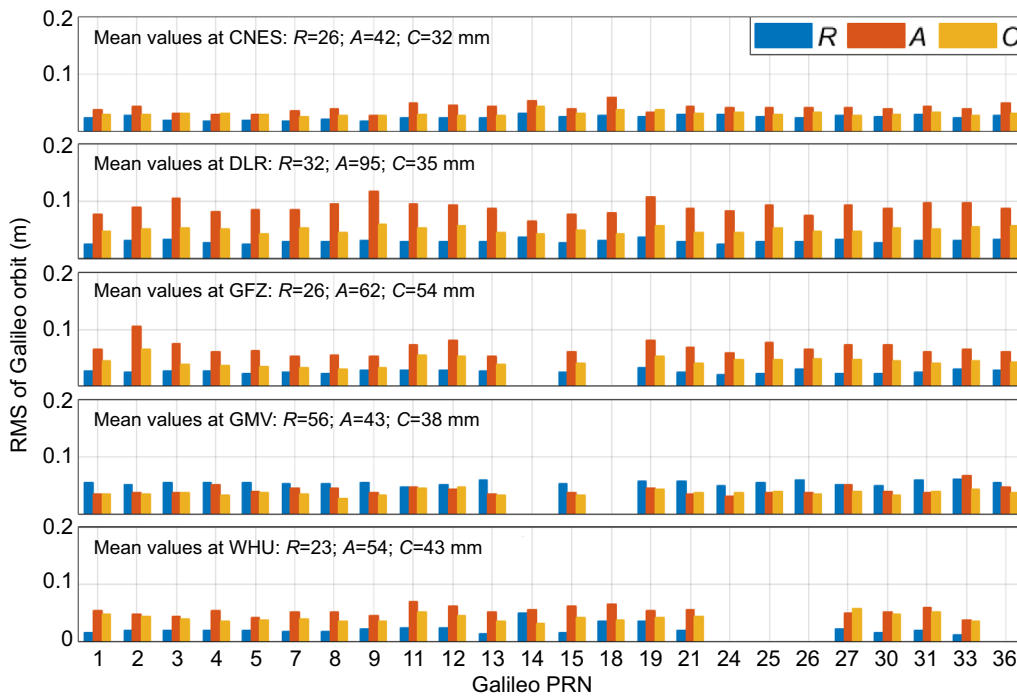
Fig. 4 RMSs in radial, along-track, and cross-track directions of Galileo real-time orbits from different ACs (mean RMS of orbit errors for all Galileo satellites is shown in each subplot)
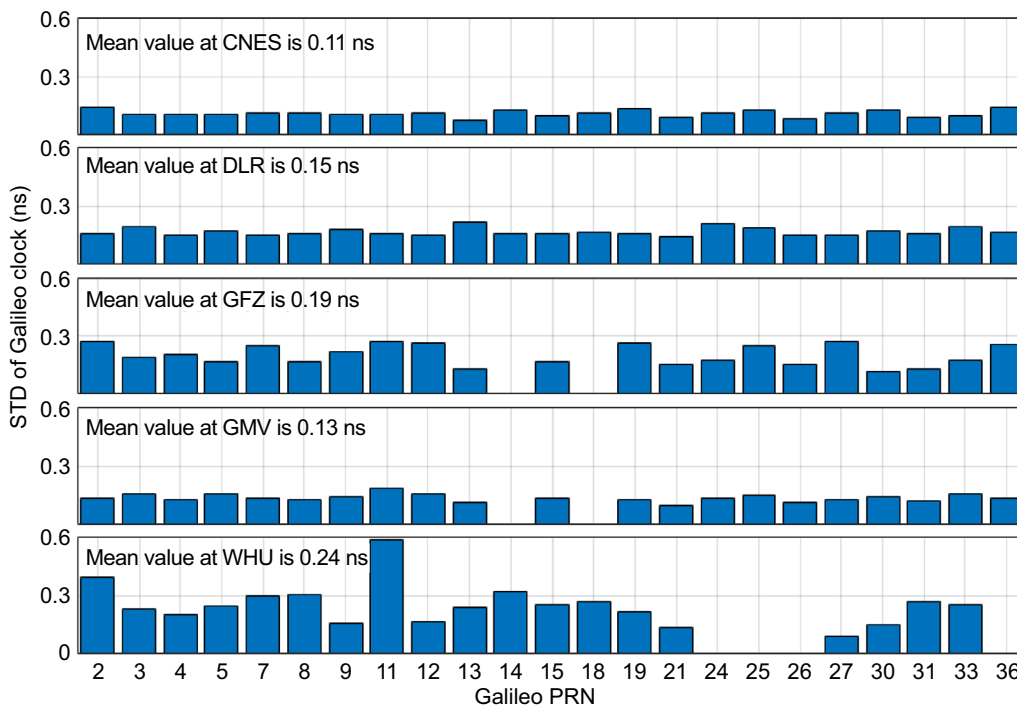
Fig. 5 STDs of real-time clock bias product of Galileo from different ACs (mean STD of clock errors for all Galileo satellites is shown in each subplot)
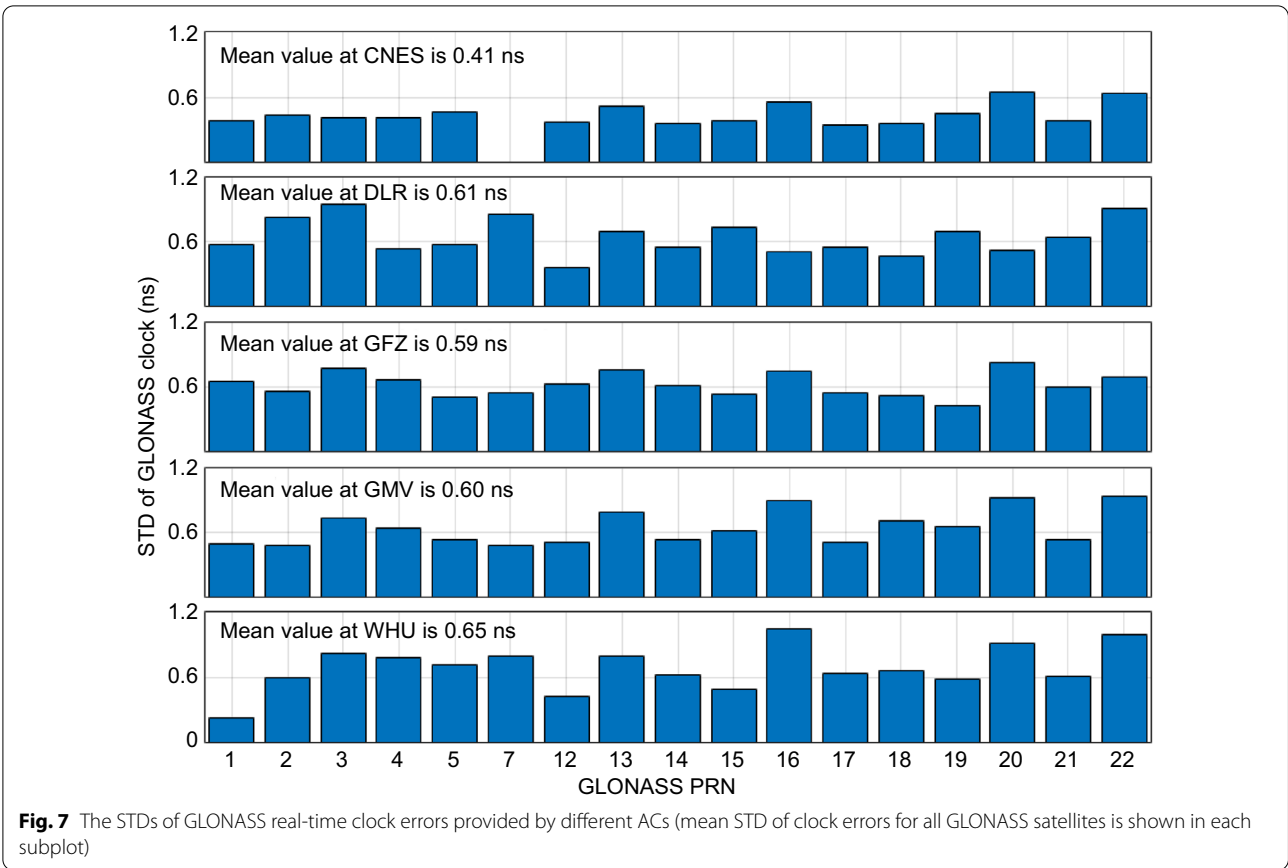
Li *et al. Satellite Navigation*   (2022) 3:12

Page 9 of 17

Fig. 6 RMSs of GLONASS orbit products in along-track, cross-track, and radial directions from different ACs (mean RMS of orbit errors for all GLONASS satellites is shown in each subplot)

Figure 10 shows the STDs of BDS-2 clock errors for GEO, IGSO, and MEO satellites. Consistent with the orbit quality, the mean STD of clock errors for GEO satellites is about 1 ns, much larger than that of IGSO and MEO satellites. The mean STD for MEO satellites is about 0.5 ns, which is larger than those of GPS and Galileo.

Figure 11 shows the STDs of clock errors for BDS-3 satellites from different ACs. In general, the precision of BDS-3 clock products is better than that of BDS-2. For MEO satellites, the STDs are 0.242 0.350 and 0.347 ns for the products from CNES, WHU, and DLR, respectively. The clock errors from C38 to C46 of WHU are relatively larger, probably due to the number of the stations used for clock error generation. Though MGEX stations provide BDS-3 observations, but most of them only observed from C19 to C37 in the testing period. After excluding MEO satellites from C41 to C46, the mean STD of WHU is reduced to 0.2616 ns, which is comparable to that of CNES. The mean STD of clock errors for BDS-3 IGSO satellites from WHU is 0.680 ns.

**Real-time PPP with real-time products from different ACs**
In order to further assess the performance of the real-time products, we carried out real-time PPP with the products. 14 well distributed MGEX stations were selected, as shown in Fig. 12. The testing period is the same as therefore, i.e., DOY 31–37 in 2021. The dual-frequency ionospheric-free model was used. In terms of the product quality for three types of BDS satellites, the weights are usually set unequal for the observations of GEO, IGSO satellites, and observations of MEO satellites (Yang et al., 2014; Zhou et al., 2018). The weights of GEO, IGSO, and MEO observations in our software are 1, 5, 15, respectively (Li et al., 2019). The coordinate parameters are modelled as random-walk with process noise of 60^2 m^2/s to simulate kinematic situation. The parameters and settings of PPP processing are presented in Table 3. Recently, Psychas et al. (2022) have demonstrated that the stochastic contribution of SSR orbit and clock corrections is quite important for real-time PPP AR. In this article, PPP float solution is adopted and the stochastic contribution of SSR corrections isn't considered yet. This could be investigated in the near future.

Fig. 7 The STDs of GLONASS real-time clock errors provided by different ACs (mean STD of clock errors for all GLONASS satellites is shown in each subplot)
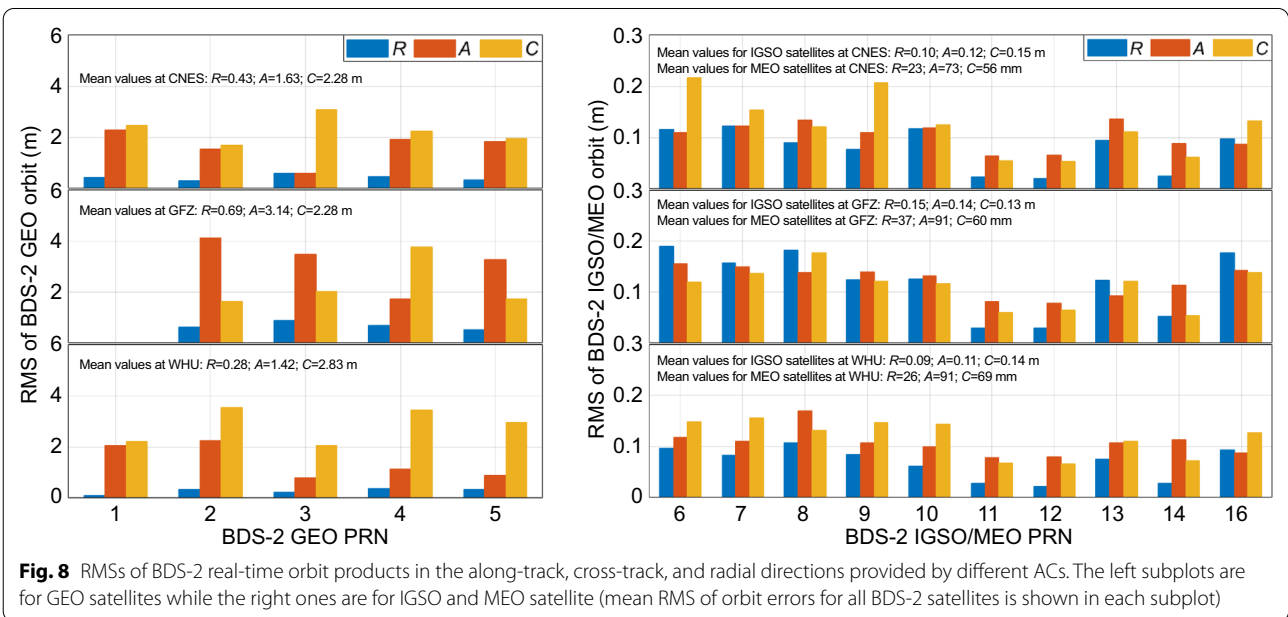

Fig. 8 RMSs of BDS-2 real-time orbit products in the along-track, cross-track, and radial directions provided by different ACs. The left subplots are for GEO satellites while the right ones are for IGSO and MEO satellite (mean RMS of orbit errors for all BDS-2 satellites is shown in each subplot)
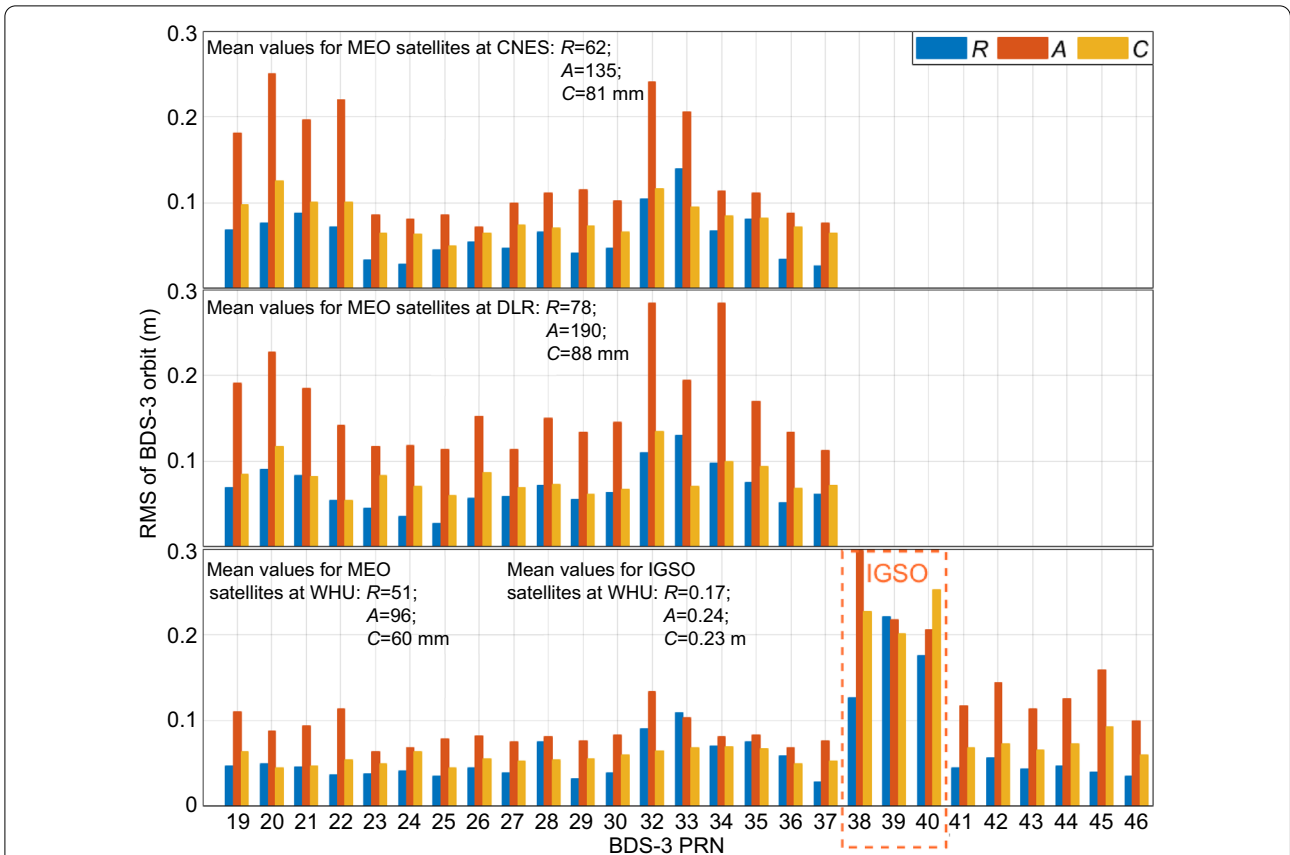
Fig. 9 RMSs of BDS-3 real-time orbit products in the along-track, cross-track, and radial from different ACs (mean RMS of orbit errors for all BDS-3 satellites is shown in each subplot; the satellites in box of dash-lines are the BDS-3 IGSO satellites)
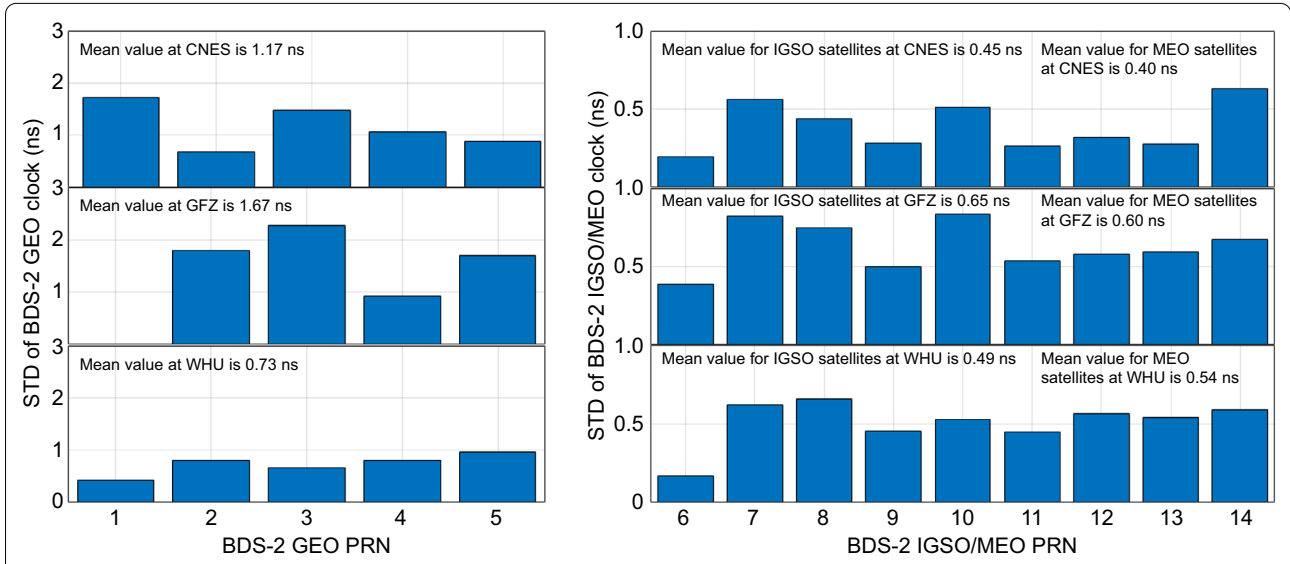
Fig. 10 STDs of BDS-2 real-time clock errors from different ACs (mean STD of clock errors for each type of BDS-2 satellites is summarized in each subplot)

Fig. 11 STDs of BDS-3 real-time clock errors from different ACs (mean STD of clock errors for all BDS-2 MEO satellites and all IGSO satellites is shown in each subplot; the satellites in the box of dash-lines are BDS-3 IGSO satellites)
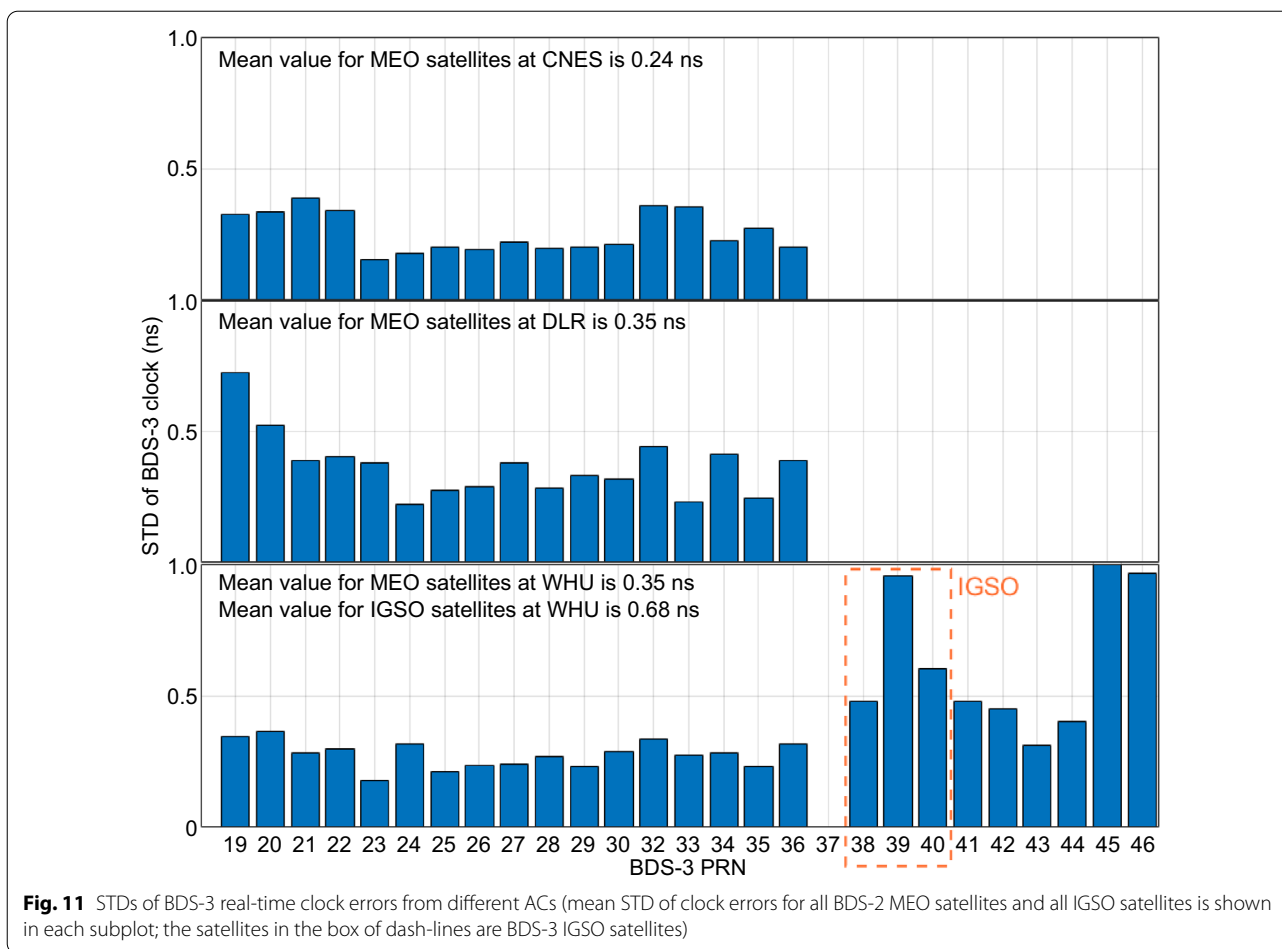
In the experiment, the software MUSIP V2.0 developed by the GNSS group in Tongji University (Li et al., 2019) was adopted for real-time kinematic PPP. The station coordinates from IGS SINEX file were used as reference (Kouba, 2009). The convergence time is defined as the first epoch (time) where the errors of east/north/up components converge to better than the thresholds of 0.1, 0.1,

Fig. 12 Distribution of 14 selected MGEX stations in the PPP experiments

0.2 m and holds for at least 60 consecutive epochs which corresponds to 30 min (Abdi et al., 2017).

Figure 13 shows the GPS real-time kinematic PPP errors by using the real-time products from each AC at station CUT0 on DOY 36, 2021. A jump at around hour 6 for IGS03 products is due to the reconvergence caused by the interruption of IGS03 GPS corrections. Overall, the GPS-only real-time kinematic PPP can converge to decimeter or even centimeter level by using the products from CNES, ESA, GFZ, and WHU.

Table 4 presents the averaged RMSs and convergence times of real-time kinematic PPP for the single system of GPS, Galileo, or BDS. Due to the quality of the products, the positioning results with DLR and IGS03 are not as good as those with other ACs. The RMS values with of DLR products are 6.94, 6.98 and 12.81 cm in east, north, and up, respectively, with convergence time of 49 min. The GPS-only positioning accuracy of GFZ is the highest with 2.48, 1.97 and 5.67 cm for east, north, and up directions, respectively. For Galileo, the positioning results of CNES and GFZ are comparable. The mean RMSs are about 4.52, 3.80 and 8.06 cm. For BDS with the
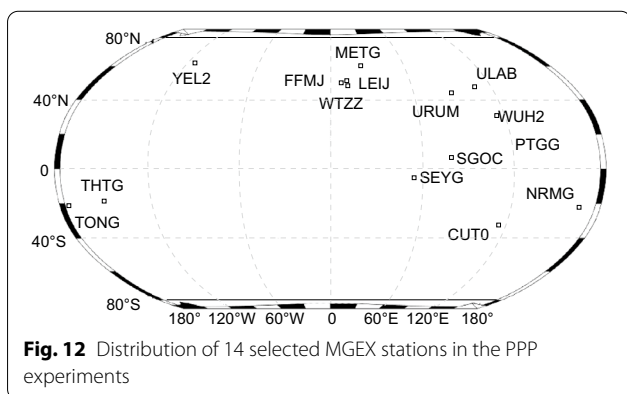
Table 3 Strategies for real-time kinematic PPP

Items	Correction model or estimation strategy
Satellites	GPS, Galileo, BDS and GLONASS
Observations	Ionosphere-free code and phase combinations
Satellite orbit and clock	Navigation message and SSR from different ACs
Sampling interval	30 s
Cutoff elevation	10°
Observation weight	Pseudo range noise: 0.5 m; Carrier phase noise: 3 mm Elevation-dependent (based on sine of elevation)
Phase-windup effect	Corrected according to Wu et al. (1992)
PCO/PCV	GPS, Galileo and GLONASS: corrected with igs14.atx (Dawidowicz, 2018) BDS only correct Phase Center Offset (PCO)
Relativistic effects	Corrected
Solid tide	International Earth Rotation and Reference Systems Service (IERS) Conventions 2010 (Petit & Luzum, 2010)
Ocean loading	IERS Conventions 2010 (Petit & Luzum, 2010)
Pole tide	IERS Conventions 2010 (Petit & Luzum, 2010)
Coordinates	Initial values are from Stand Point Positioning (SPP), process noise: 60^2 m^2 /s
Receiver clock	Initial value is from SPP, process noise: 60^2 m^2 /s
Troposphere	A priori model (Saastamoinen, 1972) and Global Mapping Function (GMF) (Boehm et al., 2006) are used and zenith wet delay is estimated as random walk noise. Initial value: 0.15 m, process noise: 1×10^{-8} m^2/s
Carrier-Phase ambiguities	Initial value: $N_j = \Phi - P + 2\frac{\lambda_j^2}{\lambda_1^2} I_1$, j denotes frequency index, process noise: 0 (i.e., as constant)
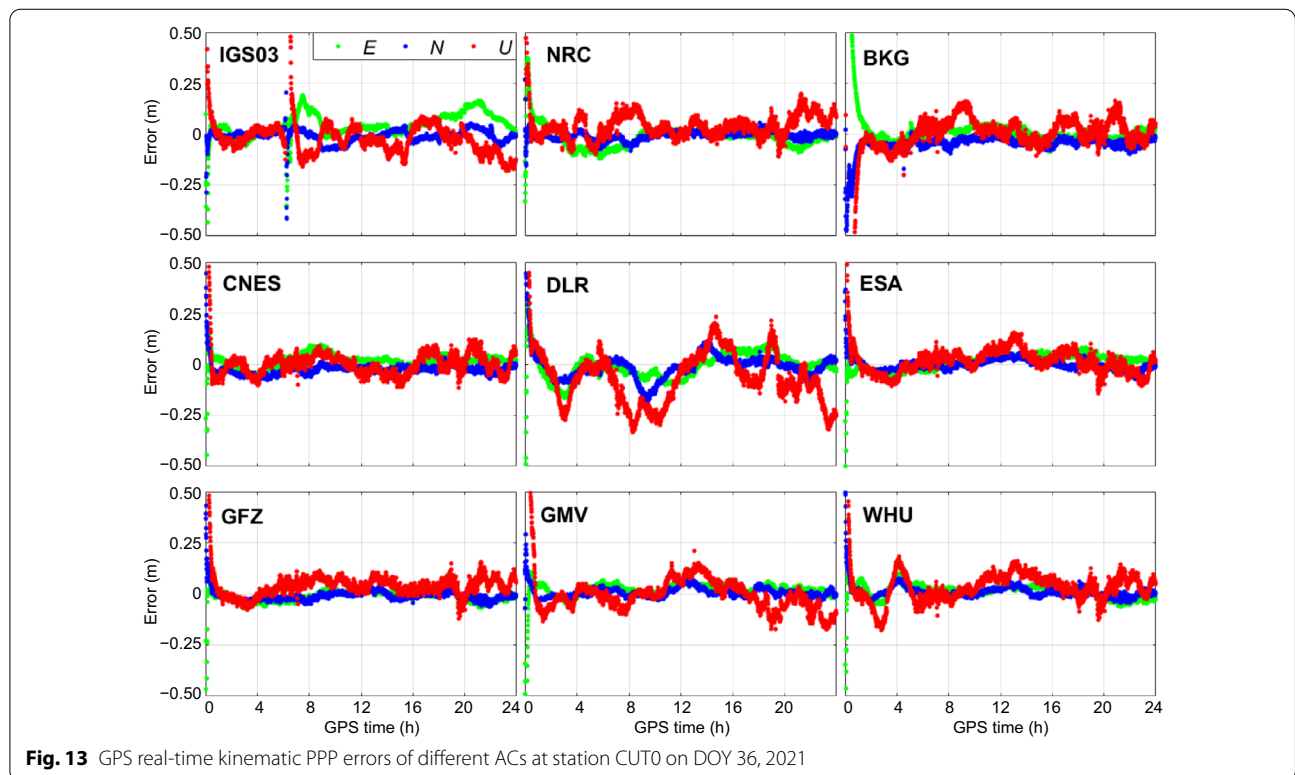
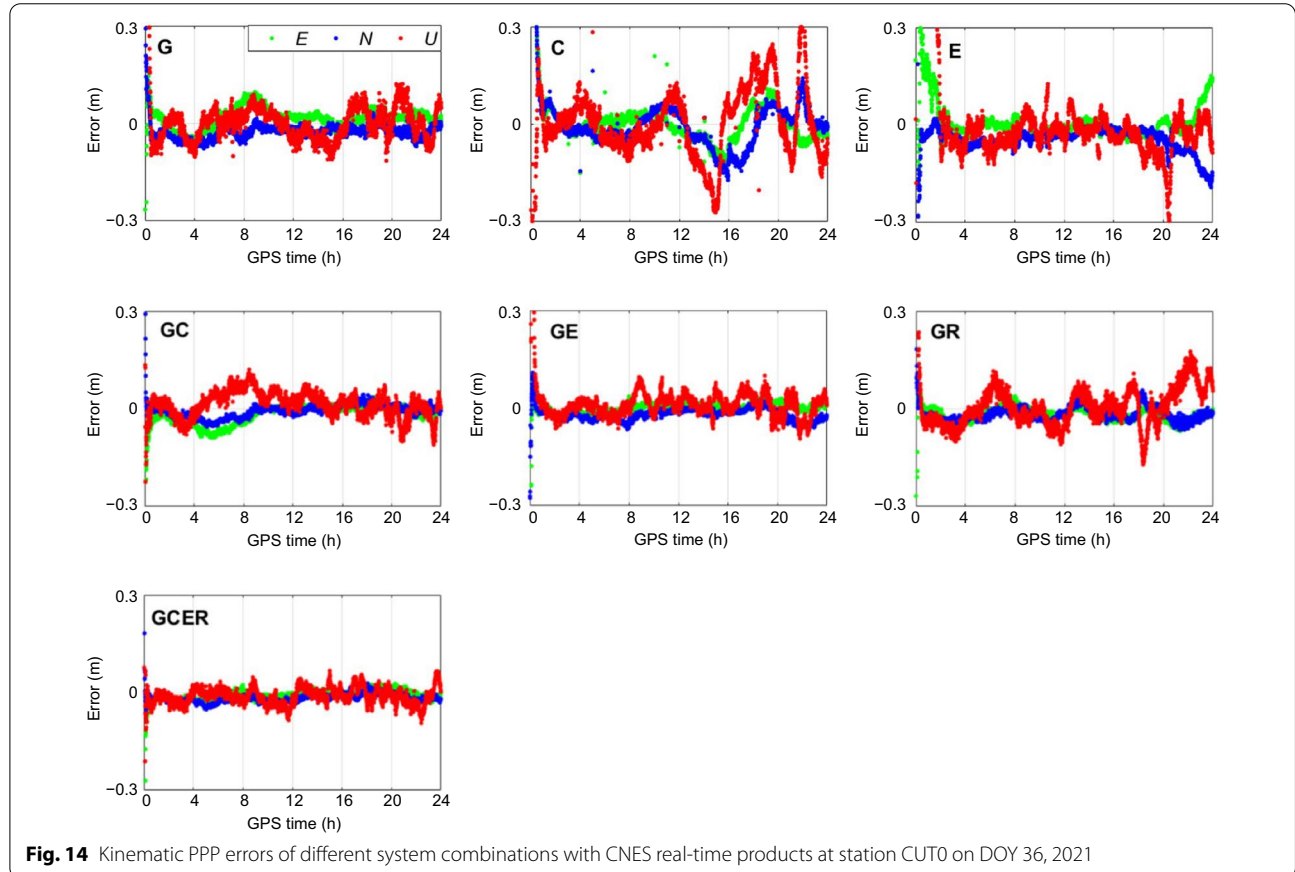**Fig. 13** GPS real-time kinematic PPP errors of different ACs at station CUT0 on DOY 36, 2021

Table 4 The averaged RMS (cm) in three coordinate components of East (*E*), North (*N*) and Up (*U*) as well as the convergence time (Abbreviated as *CT* in Table) (min) of RT kinematic single-system PPP errors for GPS, Galileo and BDS systems with the products from different ACs

AC	GPS				Galileo				BDS			
	E	*N*	*U*	*CT*	*E*	*N*	*U*	*CT*	*E*	*N*	*U*	*CT*
IGS03	6.18	5.25	12.48	38.34	–	–	–	–	–	–	–	–
NRC	3.90	3.92	8.67	40.78	–	–	–	–	–	–	–	–
BKG	4.17	3.37	6.91	69.76	–	–	–	–	–	–	–	–
CNE0	3.59	2.99	6.00	43.10	4.58	3.86	7.93	67.74	5.63	3.66	6.14	52.32
DLR	6.94	6.98	12.81	49.00	7.74	5.89	12.30	102.3	–	–	–	–
ESA	2.85	2.15	6.08	33.85	–	–	–	–	–	–	–	–
GFZ	2.48	1.97	5.67	34.80	4.45	3.74	8.12	75.17	–	–	–	–
GMV	3.40	2.29	6.51	45.38	4.79	4.03	8.76	80.63	–	–	–	–
WHU	2.79	1.91	6.41	35.37	6.78	4.62	10.13	91.14	6.43	4.45	9.31	61.4

CNES products, the mean RMSs are about 5.63, 3.66 and 6.14 cm with the convergence time of 52.32 min.

Figure 14 shows the real-time kinematic PPP errors with different system combinations by using the real-time products from CNES. The BDS-only results are unstable during hour 20–hour 24 with 0.4 m variations in height component, which is mainly due to the limited number of visible satellites as well as the quality of relevant corresponding products as described in the last section. Because of the advantages of multi-system combination, i.e., the reduced PDOP and the increased number of visible satellites, the real-time kinematic PPP errors become stable for GC, GE, GR, and GREC. In particularly, the four-system combination of GREC

Fig. 14 Kinematic PPP errors of different system combinations with CNES real-time products at station CUT0 on DOY 36, 2021

Li *et al. Satellite Navigation*   (2022) 3:12

Page 15 of 17

obtains quite stable solutions with the shortest convergence time.

Table 5 summarizes the mean RMSs and convergence times of multi-GNSS real-time kinematic PPP with GC, GE, GR, and GREC, respectively. Compared with the single system results, the multi-GNSS combination gives higher positioning accuracy and shorter convergence time. The performances of all dual-system combinations are comparable with the accuracy of about 2.1, 1.5 and 4.8 cm in east, north and up directions, respectively, and the convergence time of about 30 min for CNES, GFZ, and WHU. For GREC combination, the product of CNES gives the best results with positioning accuracy of 1.76, 1.12 and 2.68 cm in east, north, and up directions, respectively and the convergence time of about 15 min. The product of WHU is slightly worse than those of CNES. Its corresponding accuracy is 1.79, 1.54 and 2.78 cm in east, north and up directions, respectively, and the convergence time is 18.75 min. The results of DLR are worse than those of other ACs because of the poor quality of its products as aforementioned. As a comparison, the ambiguity-float multi-GNSS PPP with IGS final products usually takes about 10 min to converge to 10 cm for 2D positioning errors and the positioning accuracy is about 3 cm for 3D coordinates (Glaner and Weber, 2021). The slightly shorter convergence time and smaller positioning errors are mainly caused by the final IGS precise orbit and clock products.

Conclusions

This article evaluated the real-time orbit and clock products in SSR format from different ACs. The decoding format of real-time products and the recovery principle of real-time precise orbit and clock information were introduced. With one-week real-time products, we comprehensively evaluated the quality of the products by comparing them with GFZ precise products and their usage in kinematic PPP. The conclusions are as follows.

1. So far, total of 10 ACs provide the real-time orbit and clock SSR products. In order to further standardize the RTS service, two decoding formats, i.e., RTCM V3.x and IGS SSR Format V1.0, are applied currently for the real-time correction products.

2. All ACs provide GPS real-time products, but only some of them provide the products for four GNSSs. In general, the product quality in the order from high to low is for GPS, Galileo, BDS-3, GLONASS, and BDS-2. Regarding the comparison among ACs, both CNES and WHU provide more complete products, and the service of CNES is the most stable with highest accuracy. Overall, the accuracies of orbit products of GPS, GLONASS, Galileo, BDS MEO can reach centimeter level, while only decimeter or meter level for BDS IGSO and GEO satellites. The clock products of GPS and Galileo have the error of smaller than 0.2 ns, much better than those of BDS and GLONASS. However, the mountpoint IGS03, which

Table 5 The averaged RMS (cm) in three coordinate components of East (*E*), North (*N*) and Up (*U*) as well as the convergence time (Abbreviated as *CT* in Table) (min) of real-time multi-GNSS kinematic PPP for different ACs

Contents		CNES	DLR	GFZ	GMV	WHU
GC	*E*	3.01	4.67	2.10	–	2.52
	N	1.36	3.89	1.56	–	1.79
	U	4.32	5.74	5.33	–	4.77
	CT	27.3	39.40	22.60	–	23.42
GE	*E*	2.99	4.33	2.01	2.45	2.35
	N	1.25	3.45	1.41	1.87	1.87
	U	3.87	4.96	4.76	4.34	5.03
	CT	26.79	31.76	24.45	27.45	27.74
GR	*E*	3.23	4.55	2.13	2.87	2.45
	N	1.45	3.35	1.77	2.12	1.67
	U	4.97	5.25	5.13	5.76	6.03
	CT	29.70	35.79	27.33	28.78	29.05
GREC	*E*	1.76	3.94	1.78	–	1.79
	N	1.12	2.78	1.23	–	1.54
	U	2.68	4.23	3.64	–	2.78
	CT	15.35	28.42	19.43	–	18.75

Li *et al. Satellite Navigation*   (2022) 3:12

Page 16 of 17

is the IGS's combination of other streams, does not perform as good as other streams in testing period.

3. In terms of real-time PPP results using real-time products from different ACs, the products of CNES, GFZ, and WHU can obtain the stable PPP solutions, while the products of other ACs perform slightly worse. Regarding the GNSS systems, GPS outperforms the other systems and can give the centimeter level positioning accuracy. However, the convergence time is longer than 30 min for all single-system situations. The multi-GNSS real-time PPP can significantly improve the accuracy to 1.76, 1.12, and 2.68 cm in east, north, and up directions, respectively and shorten the convergence time to 15 min.

Availability of data and materials
The datasets used and/or analyzed during the current study are freely downloaded from the websites mentioned in the manuscript.

Declarations

Competing interests
The authors declare that they have no competing interests.

References

Abdi, N., Ardalan, A. A., Karimi, R., & Rezvani, M. H. (2017). Performance assessment of multi-GNSS real-time PPP over Iran. *Advances in Space Research, 59*(12), 2870–2879.

Bedford, J. R., Moreno, M., Deng, Z., Oncken, O., Schurr, B., John, T., Baeez, J. C., & Bevis, M. (2020). Month-long thousand-kilometre-scale wobbling before great subduction earthquakes. *Nature, 580*, 628–635.

Boehm, J., Niell, A., Tregoning, P., & Schuh, H. (2006). Global mapping function (GMF): A new empirical mapping function based on numerical weather model data. *Geophysical Research Letters, 33*(7), L07304.

Boisits, J., Glaner, M., & Weber, R. (2020). Regiomontan: A regional high precision ionosphere delay model and its application in precise point positioning. *Sensors., 20*(10), 2845.

Cai, C., Gao, Y., (2007). Performance analysis of precise point positioning based on combined GPS and GLONASS. In Proc: ION GNSS 2007, Fort Worth, TX, USA, 25–28 September 2007. pp: 858–865.

Chen, K., Liu, Z., & Song, T. (2020). Automated GNSS and teleseismic earthquake inversion (AutoQuake Inversion) for tsunami early warning: retrospective and real-time results. *Pure and Applied Geophysics, 177*(1), 1403–1423.

Chen, X. (2020). An alternative integer recovery clock method for precise point positioning with ambiguity resolution. *Satellite Navigation, 1*(1), 1–9.

China Satellite Navigation Office (CSNO) (2016). BeiDou Navigation Satellite System Signal in Space Interface Control Document Open Service Signal (Version 2.1).

Collins, P., (2008). Isolating and estimating undifferenced GPS integer ambiguities. In: Proc ION NTM, January 28–30. San Diego, California, USA. pp 720–732.

Dai, X., Ge, M., Lou, Y., Shi, C., Wickert, J., & Schuh, H. (2015). Estimating the yaw-attitude of BDS IGSO and MEO satellites. *Journal of Geodesy, 89*(10), 1005–1018.

Dawidowicz, K. (2018). IGS08.ATX to IGS14.ATX change dependent differences in a GNSS-derived position time series. *Acta Geodynamica ET Geomaterialia, 15*(4), 363–378.

de Bakker, P. F., & Tiberius, C. C. J. M. (2017). Real-time multi-GNSS single-frequency precise point positioning. *GPS Solut., 21*(4), 1791–1803.

Deng, Z., Thomas, N., & Markus, B. (2017). Multi-GNSS Rapid Orbit-. *Clock- & EOP-Product Series. GFZ Data Services.* https://doi.org/10.5880/GFZ.1.1.2017.002

Elsobeiey, M., & Al-Harbi, S. (2016). Performance of real-time precise point positioning using IGS real-time service. *GPS Solutions, 20*(3), 565–571.

European Union (EU) (2010). European GNSS (Galileo) open service: signal in space interface control document. Office for Official Publications of the European Communities.

Ge, M., Gendt, G., Rothacher, M., Shi, C., & Liu, J. (2008). Resolution of GPS carrier-phase ambiguities in precise point positioning (PPP) with daily observations. *Journal of Geodesy, 82*, 389–399.

Geng, J., & Bock, Y. (2013). Triple-frequency GPS precise point positioning with rapid ambiguity resolution. *Journal of Geodesy, 87*, 449–460.

Glaner, M., & Weber, R. (2021). PPP with integer ambiguity resolution for GPS and Galileo using satellite products from different analysis centers. *GPS Solution, 25*(3), 1–13.

IGS RTWG (2020) IGS state space representation (SSR) format version 1.00.

Kazmierski, K., Sosnica, K., & Hadas, T. (2018). Quality assessment of multi-GNSS orbits and clocks for real-time precise point positioning. *GPS Solutions, 22*(1), 11.

Keshin MO, Le AQ, Marel H (2006) Single and dual-frequency precise point positioning: approaches and performance, Proceedings of the 3rd ESA Workshop on Satellite Navigation User Equipment Technologies, Noordwijk, pp 11–13

Kouba J (2009) A guide to using International GNSS Service (IGS) products.

Krzan, G., & Przestrzelski, P. (2016). GPS/GLONASS precise point positioning with IGS real-time service product. *Acta Geodynamica Et Geomaterialia., 13*(1), 69–81.

Laurichesse D., Mercier F. (2007). Integer ambiguity resolution on undifferenced GPS phase measurements and its application to PPP. In: Proceedings ION GNSS 2007, 25–28 Semptember, Fort Worth, TX, USA. pp, 839–848.

Laurichesse., D, Mercier., F, Berthias., J.P., (2009). Real Time GPS Constellation and Clocks Estimation using Zero-difference Integer Ambiguity Fixing. In Proc: ION ITM 2009, January 26–28, 2009. Anaheim, California, USA. pp: 664–672.

Li, B., Shen, Y., & Feng, Y. (2010). Fast GNSS ambiguity resolution as an ill-posed problem. *Journal of Geodesy, 84*, 683–698.

Li, B., Zang, N., Ge, H., & Shen, Y. (2019). Single-frequency PPP models: Analytical and numerical comparison. *Journal of Geodesy, 93*, 2499–2514.

Li, X., Liu, G., Li, X., Zhou, F., Feng, G., Yuan, Y., & Zhang, K. (2020). Galileo PPP rapid ambiguity resolution with five-frequency observations. *GPS Solutions, 24*, 24.

Li *et al. Satellite Navigation*   *(2022) 3:12*

Page 17 of 17

Li, X., Zhang, X., Ren, X., Fritsche, M., Wickert, J., & Schuh, H. (2015). Precise positioning with current multi-constellation Global Navigation Satellite Systems: GPS, GLONASS. *Galileo and BeiDou. Sciences Reports, 5*, 8328.

Liu, T., Wang, J., Yu, H., Cao, X., & Ge, Y. (2018). A new weighting approach with application to ionospheric delay constraint for GPS/GALILEO real-time precise point positioning. *Applied Sciences, 8*(12), 2537.

Liu, T., Yuan, Y., Zhang, B., Wang, N., Tan, B., & Chen, Y. (2017). Multi-GNSS precise point positioning (MGPPP) using raw observations. *Journal of Geodesy, 91*(3), 253–268.

Lou, Y, (2008). Research on real-time precise GPS orbit and clock offset determination. Wuhan University.

Montenbruck, O., Steigenberger, P., Prange, L., Deng, Z., Zhao, Q., Perosanz, F., Romero, I., Noll, C., Stuerze, A., Weber, G., Schmid, R., Macleod, K., & Schaer, S. (2017). The multi-GNSS experiment (MGEX) of the international GNSS service (IGS)–achievements, prospects and challenges. *Advances in Space Research, 59*(7), 1671–1697.

Odijk, D., Zhang, B., Khodabandeh, A., Odolinski, R., & Teunissen, P. (2016). On the estimability of parameters in undifferenced, uncombined GNSS network and PPP-RTK user models by means of S-system theory. *Journal of Geodesy, 90*, 15–44.

Petit., G, Luzum., B, (2010). IERS Conventions, IERS Technical Note No.36, Verlag des Bundesamts für Kartographie und Geodäsie, Frankfurt am Main.

Psychas, D., Khodabandeh, A., & Teunissen, P. J. G. (2022). Impact and mitigation of neglecting PPP-RTK correctional uncertainty. *GPS Solut., 26*(1), 1–15.

RTCM Special Committee (2016). RTCM standard 10403.3 differential GNSS (global navigation satellite systems) services-version 3. RTCM Special Committee, (104).

Saastamoinen, J. (1972). Atmospheric correction for the troposphere and stratosphere in radio ranging of satellites. The use of artificial satellites for geodesy. *American Geophysics Union Geophysics Monograph Series, 15*, 247–251.

Standard RTCM (2011). 10410.1 for Networked Transport of RTCM via internet protocol. V2 June.

Teunissen, P. J. G., Odijk, D., & Zhang, B. (2010). PPP-RTK: Results of CORS network-based PPP with integer ambiguity resolution. *J Aeronautics, Astronautics Aviation, 42*(4), 223–229.

Wang, C., Guo, J., Zhao, Q., & Liu, J. (2019). Empirically derived model of solar radiation pressure for BeiDou GEO satellites. *Journal of Geodesy, 93*(6), 791–807.

Wang, L., Li, Z., Ge, M., Neitzel, F., Wang, Z., & Yuan, H. (2018a). Validation and assessment of multi-GNSS real-time precise point positioning in simulated kinematic mode using IGS real-time service. *Remote Sensors, 10*(2), 337.

Wang, Z., Li, Z., Wang, L., Wang, X., & Yuan, H. (2018b). Assessment of multiple GNSS real-time SSR products from different analysis centers. *ISPRS International Journal of Geo-Information, 7*(3), 85.

Weber., G, Mervart., L, Lukes., Z, Rocken., C, Dousa., J (2007). Real-time clock and orbit corrections for improved point positioning via NTRIP. In Proc: ION GNSS, Fort Worth, TX, USA, pp 1992–1998.

Wu, J., Wu, S., Hajj, G., Bertiger, W., & Lichten, S. (1992). Effects of antenna orientation on GPS carrier phase. *Manuscr Geod., 18*(2), 91–98.

Xin, S., Geng, G., Guo, G., & Meng, X. (2020). On the choice of the third-frequency galileo signals in accelerating PPP ambiguity resolution in case of receiver antenna phase center errors. *Remote Sensor, 12*, 1315.

Yang, Y., Li, J., Wang, A., Xu, J., He, H., Guo, H., Shen, J., & Dai, X. (2014). Preliminary assessment of the navigation and positioning performance of BeiDou regional navigation satellite system. *Science China Earth Sciences., 57*(1), 144–152.

Zhang, Z., Li, B., Nie, L., Wei, C., Jia, S., & Jiang, S. (2019). Initial assessment of BeiDou-3 global navigation satellite system: Signal quality, RTK and PPP. *GPS Solutions, 23*(4), 1–12.

Zhang, B., Hou, P., Zha, J., & Liu, T. (2022). PPP–RTK functional models formulated with undifferenced and uncombined GNSS observations. *Satellite Navigation, 3*(1), 1–15.

Zhang, L., Yang, H., Gao, Y., Yao, Y., & Xu, C. (2018). Evaluation and analysis of real-time precise orbits and clocks products from different IGS analysis centers. *Advances in Space Research, 61*(12), 2942–2954.

Zhao, Q., Wang, C., Guo, J., Wang, B., & Liu, J. (2017). Precise orbit and clock determination for BeiDou-3 experimental satellites with yaw attitude analysis. *GPS Solutions, 22*, 4.

Zhou, F., Dong, D., Li, W., Jiang, X., Wickert, J., & Schuh, H. (2018). GAMP: An open-source software of multi-GNSS precise point positioning using undifferenced and uncombined observations. *GPS Solutions, 22*, 33.

Zumberge, J. F., Heflin, M. B., Jefferson, D. C., Watkins, M. M., & Webb, F. H. (1997). Precise point positioning for the efficient and robust analysis of GPS data from large networks. *Journal of Geophysical Research: Solid Earth, 102*, 5005–5017.

Publisher's Note